Title

RNA-antimicrobial peptide complexes fuel a TLR- and NETosis-mediated inflammatory cycle of neutrophil activation in psoriasis

Running title

RNA and LL37 activate neutrophils in psoriasis

Authors

Franziska Herster[1], Zsofia Bittner[1], Sabine Dickhöfer[1], David Eisel[1,$], Tatjana Eigenbrod[2], Thomas Knorpp[3], Nicole Schneiderhan-Marra[3], Markus W. Löffler[1,4], Dominik Hartl[5], Lukas Freund[6], Knut Schäkel[6], Martin Heister[7], Kamran Ghoreschi[7], Alexander N.R. Weber[1,*]

Affiliations

[1] Department of Immunology, University of Tübingen, Auf der Morgenstelle 15, 72076 Tübingen, Germany

[2] Department of Infectious Diseases, Medical Microbiology and Hygiene, University Hospital Heidelberg, Im Neuenheimer Feld 324, 69120 Heidelberg, Germany

[3] NMI Natural and Medical Sciences Institute at the University of Tübingen, Markwiesenstr. 55, 72770 Reutlingen, Germany

[4] Department of General, Visceral and Transplant Surgery, University Hospital Tübingen, Hoppe-Seyler-Str. 3, 72076 Tübingen, Germany

[5] University Children's Hospital and Interdisciplinary Center for Infectious Diseases, University of Tübingen, Hoppe-Seyler-Str. 1, 72076 Tübingen, Germany

[6] Department of Dermatology, University Hospital Heidelberg, Im Neuenheimer Feld 440, 69120 Heidelberg, Germany

[7] Department of Dermatology, University Hospital Tübingen, Liebermeisterstr. 25, 72076 Tübingen, Germany

*** Contact information (Corresponding Author)**

Alexander N. R. Weber, Interfaculty Institute for Cell Biology, Department of Immunology, University of Tübingen, Auf der Morgenstelle 15, 72076 Tübingen, Germany. Tel.: +49 7071 29 87623. Fax: +49 7071 29 4579. Email: alexander.weber@uni-tuebingen.de

[$] Change of address/additional addresses

David Eisel, GMP & T Cell Therapy Unit (G183), German Cancer Research Center, Im Neuenheimer Feld 280, 69120 Heidelberg, Germany

Dominik Hartl, Galapagos Pharma, Basel, Switzerland

Keywords

Antimicrobial peptide LL37, RNA, psoriasis, neutrophil, Toll-like receptor (TLR), neutrophil extracellular trap (NET)

Key points

Human and bacterial RN in complexed with LL37 activates neutrophils via TLR8 to release cytokines, chemokines and neutrophil extracellular traps (NETs);

NETs and neutrophil-rich areas in psoriatic skin contain RNA and LL37, suggesting RNA+LL37 may fuel a PMN-mediated and self-sustaining inflammatory cycle in psoriasis.

Abstract

Psoriasis is an inflammatory autoimmune disease characterized by skin lesions showing strong neutrophil (PMN) infiltration and high levels of the antimicrobial peptide, LL37, but the role of PMNs in this context remains unclear. We here show that primary human PMNs, especially PMNs from psoriasis patients, not only respond via TLR8 to human and bacterial RNA in complexed with LL37 by cytokine-, chemokine- and neutrophil extracellular trap (NET)-release; they also actively release additional RNA and LL37 in response to stimulation by the same complex and both RNA and LL37 were found to be highly abundant in psoriatic skin. RNA-LL37 complexes can thus fuel a PMN-mediated and self-sustaining inflammatory loop that may represent an unexpected early initiator or amplifying event in psoriasis. Given that TLR inhibitory oligodeoxynucleotides prevent the activation of PMNs by RNA-LL37 complexes *in vitro*, our study also highlights TLR blockade as a potential therapeutic intervention strategy in psoriasis.

Psoriasis is an autoimmune disease of the skin with high incidence in Western countries (1.5-3%), causing high socioeconomic and disease burden with limited but increasing treatment options [1, 2]. The most common form of psoriasis, plaque psoriasis, is characterized by epidermal hyperplasia due to keratinocyte (KC) hyper-proliferation, increased endothelial proliferation and an infiltrate of leukocytes, such as dendritic cells, T cells and, prominently, polymorphonuclear neutrophils (PMNs) [1]. The high and early accumulation of PMNs in psoriatic plaques and micro-abscesses is well documented, as well as an increase of PMNs in the circulation of psoriasis patients [3 4]. However, it is unclear whether PMN infiltration represents a bystander phenomenon or has a causal role in the development of the disease.

PMNs are known as a source of LL37, an amphipathic, positively-charged 37 amino acid peptide generated from a precursor protein, the cathelicidin hCAP18, and highly abundant in psoriatic lesions [1, 5]. LL37 is stored in the secondary granules of PMNs, from which it can be released upon activation [6]. Apart from acting as a self-antigen for CD4 helper T cells in psoriasis patients [7], LL37 was previously shown to form complexes with DNA or RNA that resisted nuclease degradation, were readily taken up by plasmacytoid dendritic cells (pDCs), and triggered high Interferon (IFN) α and low Tumor necrosis factor (TNF) or Interleukin (IL) 6 secretion from these cells [8, 9]. Although type I IFNs contribute to psoriasis [10, 11], chemokines and pro-inflammatory cytokines such as TNF, IL-1β or IL-23 are additionally required for immune cell infiltration and T cell polarization, respectively [12]. Since pDCs are comparatively low producers of these psoriasis-initiating inflammatory cytokines and do not accumulate to high numbers in psoriatic skin, this raises the question whether nucleic acid-LL37 sensing by other immune cells, particularly PMNs, may contribute more prominently to initial inflammatory cytokine/chemokine milieu observed in psoriasis.

In contrast to pDCs, PMNs are known producers of considerable amounts of various cytokines and chemokines [13, 14, 15]. Additionally, PMNs are able to undergo neutrophil extracellular trap (NET) formation (NETosis), an activation-induced process leading to the extrusion of nuclear DNA [16], as well as cellular proteins, including LL37 [17]. Like pDCs, PMNs express multiple pattern recognition receptors (PRRs) of the Toll-like receptor (TLR) family, namely TLR2, 4, 8 [18] and 9 [19], but not TLR3 or TLR7 [18]. TLRs directly bind activating ligands, typically so-called microbe-associated molecular patterns (MAMPs) absent from the host [20]; however, when they can gain access to endosomal compartments - for example by complex formation with LL37 - host nucleic acids are able to trigger the endosomal TLRs 3, 7, 8 (sensing double-stranded or single-stranded RNA, respectively) or TLR9 (sensing DNA). TLR7 expression in humans is restricted to pDC and (only inducibly) to B cells. TLR8 thus appears to be the primary receptor for foreign (and potentially host-derived) single-stranded RNA in humans [21].

PMNs theoretically combine the abilities (i) to release LL37 and nucleic acids as components of immuno-stimulatory ligands via NETosis; (ii) to potentially sense such ligands via TLRs; and (iii) to secrete chemo-/cytokines. These mechanisms were never shown to act in concert but we speculated whether LL37-mediated DNA or RNA sensing via TLRs in PMNs might initiate and fuel inflammatory chemo-/cytokine production and thus inflammation and immune cell infiltration in psoriatic skin. We here present experimental evidence that human primary PMNs readily respond to RNA-LL37 complexes, but not RNA alone, leading to the release of a broad array of chemokines and cytokines – a process that induces chemoattraction of other immune cells and that is elevated in psoriasis patients and can be therapeutically blocked by inhibitory oligodeoxynucleotides (iODNs). Unexpectedly, RNA-LL37 also triggered the release of NETs, which contained additional LL37, RNA and DNA, thereby providing the basis for a self-propagating inflammatory cycle.

Results

LL37 promotes RNA uptake and induces TLR8-mediated PMN activation

Previous results indicated that human primary PMNs can respond to RNA and DNA when stimulated for >12 h, albeit at much lower levels than when stimulated with the nucleoside analog TLR7/8 agonist, R848 [19, 22]. We sought to re-evaluate these findings using highly purified primary PMNs assayed within a short time period (4 h) that excludes secondary release effects, e.g. by apoptosis (Fig. S1A). The TLR7/8 agonist R848, like the TLR4 agonist, LPS, elicited robust IL-8 release but only LPS triggered CD62L shedding; phospho-thioate (PTO) synthetic CpG ODN, a typical TLR9 agonist, also strongly activated IL-8 release and CD62L shedding (Fig. 1A, Table S1). However, unmodified, natural phospho-diester DNA ODN or human genomic DNA elicited neither IL-8 release nor CD62L shedding, irrespective of whether they were complexed with LL37 (Fig. 1B). In contrast, in pDC LL37 binding of natural DNA triggered potent TLR9 responses [8]. In the absence of LL37, single-stranded synthetic RNA40 (henceforward referred to as 'RNA') barely caused IL-8 release when applied at equimolar concentrations with R848 (Fig. 1C). This suggests that on their own neither RNA nor DNA are able to trigger primary PMN responses. This may be due to the endosomal localization of TLR8 and 9, which R848 and CpG can apparently access, whereas RNA and normal DNA cannot [23]. However, robust IL-8 release and moderate CD62L shedding were observed when RNA was complexed with LL37 (Fig. 1C). To check whether PMNs could engage RNA-LL37 complexes, live PMNs were seeded and RNA-LL37 complexes added for 20 min before fixing the cells for electron microscopy analysis. As shown in Fig. 1D, PMNs were found in proximity to fiber-like structures corresponding to RNA-LL37 complexes [24]. Flow cytometry using AlexaFluor (AF) 647-labeled RNA showed that LL37 also promoted the uptake of complexed RNA: >20% of PMNs incubated with labeled RNA in the presence of LL37 were AF647-positive within 60 min, compared to 5% in the absence of LL37 (Fig. 1E). ImageStream bright-field cytometry confirmed that this was not due to external/surface binding of labeled RNA but rather internalization (Fig. 1F, G). Bright-field fluorescence microscopy with Atto488-labeled LL37 showed co-localization of AF647-RNA and Atto488-LL37 in intracellular compartments (Fig. 1H) where TLR8 is expressed [18]. To confirm the role of the endosomal TLR8 pharmacologically, we investigated the effect of chloroquine, a well-known inhibitor of endosomal TLRs that was non-toxic for PMNs (Fig. S1B). Indeed IL-8 release from primary PMNs in response to RNA-LL37 and CpG ODN (positive control) was significantly reduced by chloroquine addition (Fig. 1I and S1C). Since TLR7 is not expressed in PMNs [18] and chloroquine does not affect cytoplasmic RNA sensors (e.g. RIG-I) [25], we conclude TLR8 to be the receptor mediating the observed effects in PMNs. We next sought to check whether the observed effect on cytokine release extended to normal RNA from mammalian cells which may be more physiologically relevant in the context of psoriasis. As shown in Fig. 1J, human

mRNA significantly induced IL-8 release, but only in combination with LL37. Since microbiome analyses have recently revealed alterations in staphylo- and streptococcal skin colonization in psoriasis patients [26] and bacterial RNA is an emerging immuno-stimulatory pattern [27], we also tested whether LL37 promoted *S. aureus*, i.e. bacterial RNA (bRNA) activation of PMNs. Fig. 1K shows that bRNA significantly stimulated IL-8 release similarly to RNA40 when complexed with LL37. In murine PMN this response to bRNA+LL37 (and the control stimulus R848) was strictly dependent on *Unc93b1* (Fig. S1D), a critical chaperone of endosomal TLRs [28]. Taken together this suggests that uptake of RNA is promoted by LL37 and directs RNA to intracellular compartments from which TLR8 sensing and activation leading to cytokine release can occur – both in response to mammalian and bacterial/foreign RNA.

RNA-LL37 complexes prompt release of multiple pro-inflammatory cytokines and chemokines

To test whether RNA-LL37 also promoted the release of cytokines other than IL-8, we screened supernatants of stimulated PMNs by Luminex multiplex analysis and detected TNF, IL-1β, IL-6, and – unexpectedly – IL-16 and MIP-1β primarily or exclusively in RNA-LL37-stimulated cell supernatants, respectively (Fig. S2). Despite considerable variation between donors, this was confirmed by cytometric bead arrays analyses (Fig. 2A-C) and ELISA (Fig. 2D, E) in samples from more donors. To our knowledge, active receptor-mediated release of the chemoattractants, IL-16 (also known as Lymphocyte Chemoattractant Factor, LCF) and MIP-1β (also known as Chemokine (C-C motif) Ligand, CCL4) from primary human PMNs has not been reported. In fact, release of IL-16 was also boosted by LL37 alone (Fig. 2D) and MIP-1β was strongly released from PMNs in response to RNA-LL37 complexes but not RNA alone (Fig. 2E). We conclude that the combination of RNA with LL37 can stimulate not only IL-8 release from primary PMNs; it also induced additional pro-inflammatory cytokines and chemoattractants not triggered by RNA alone.

To test whether this was relevant for the psoriasis context, we next analyzed cyto-/chemokine release in response to RNA-LL37 complexes in PMNs from patients with moderate to severe psoriasis (here referred to as 'psoriasis PMNs') without systemic treatment and a psoriasis area and severity (PASI) score ≥10. Additionally, the effect of PMN-produced cytokines on the attraction of additional immune cells known to infiltrate psoriatic skin and to contribute to pathogenesis was tested.

Psoriasis PMNs respond more potently to RNA-LL37 complexes

When repeating the above described stimulation experiments with psoriasis PMNs compared to PMNs from healthy donor, both IL-8 and MIP-1β release was increased two-fold higher in response to RNA-LL37 (Fig. 3A, B). Whereas IL-8 release in response to 'RNA alone' (i.e. without LL37) was indistinguishable from 'unstimulated' samples in healthy donor PMNs (*cf.* also Fig. 2), psoriasis PMNs treated with 'RNA alone' (Fig. 3A, arrow) produced more IL-8 than both 'unstimulated' psoriasis

PMNs and healthy donor PMNs stimulated with 'RNA alone'. Since in healthy donors, RNA seemed to strongly depend on LL37 for efficient PMN uptake and stimulation (*cf.* Fig. 1) and PMNs are the major contributors to elevated LL37 in psoriasis, we speculated whether psoriasis PMNs might constitutively secrete LL37 and this endogenous LL37 might promote an increased responsiveness to exogenously added RNA alone in psoriasis PMNs. We indeed observed that psoriasis PMNs constitutively showed an increased baseline release of LL37 compared to healthy donors (Fig. 3C) but were not pre-activated prior to stimulation (no CD62L shedding observable). The IL-8 response of psoriasis PMNs to LPS was elevated, albeit not significantly, and both psoriasis PMNs and PMNs from healthy donors produced the same levels of MIP-1β in response to LPS (Fig. S3A, B). Thus, in psoriasis PMNs TLR-mediated inflammatory mediator release was especially increased for RNA and potentially due to a higher abundance of PMN-derived LL37.

RNA-LL37 complexes induce migration of mononuclear immune cells

IL-16 is a known modulator and chemoattractant for CD4 T cells [29, 30] and MIP-1β acts as a chemoattractant for a variety of immune cells and stimulates further pro-inflammatory cytokine production [31]. We therefore next checked whether IL-16 or MIP-1β, at the concentrations observed in this study, could influence the migration and infiltration of additional immune cells, which is a hallmark of psoriatic plaques [4]. Transwell experiments with peripheral blood mononuclear cells (PBMCs) from healthy human donors (upper well) and IL-16 (300 and 1500 pg/ml), MIP-1β (30 and 150 pg/ml) or SDF-1α as a control (lower well) were conducted (Fig. 4A, B and S4). We specifically focused on T cells as known mediators of the psoriatic Th17 phenotype [12] and CD14 MHC class II (HLA-DR)-expressing monocytes as inflammatory cells and potential APCs for LL37 [7]. As shown in Fig. 4A-C, the lowest concentration of both cytokines led to a donor-dependent increase in the number of $CD3^+CD4^+$ helper, $CD3^+CD8^+$ cytotoxic T cells as well as $CD14^+HLA\text{-}DR^+$ monocytes. Possibly due to a non-linear dose response relationship observed for some cytokines [32], higher concentrations had a weaker effect. Owing to the donor-to-donor variation observed throughout in the human system, only a non-significant, moderate effect of MIP-1β was observed (Fig. 4C). We separately tested whether RNA or RNA-LL37 in the lower chamber had any direct influence on the migration of these cell populations and noted an unexpected and significant chemoattractive effect on $CD4^+$ T cells, and to a lesser extent on $CD8^+$ T cells and $CD14^+HLA\text{-}DR^+$ monocytes, in response to RNA-LL37. Interestingly, the presence of PMNs, regardless of stimulus, was sufficient to attract a variety of other cells (results not shown) due to a so far unknown mechanism. Taken together PMN-derived IL-16 and MIP-1β or RNA-LL37 complexes themselves may contribute to cellular migration of T cells and monocytes with APC capacity.

RNA-LL37 complexes trigger the release of RNA- and LL37-containing NETs

Our data so far indicate that RNA and LL37 might contribute to cytokine-mediated inflammation and immune infiltration in neutrophil-containing skin. Such neutrophil responses would probably be temporary, unless RNA-LL37 triggered the release of additional RNA and LL37. PMN NETs are known to contain extracellular DNA that acts as an immune stimulant when in complex with LL37 [33]. But DNA-LL37 cannot activate PMNs (*cf.* Fig. 1B) and RNA release by NETosis has not been shown. NETs would thus only propagate PMN activation in case they also contained RNA. We therefore tested (i) whether RNA-LL37 induces NETosis and (ii) whether NETs contain RNA. Interestingly, a neutrophil elastase-based NET assay (see Methods) also confirmed significant neutrophil elastase release, another hallmark of NETosis, in response to RNA-LL37 and PMA (positive control), but also with LL37 alone (Fig. 5A). However, fluorescence microscopy analysis of fixed PMN samples established that only RNA-LL37 complexes, and not LL37 alone, prompted the formation of LL37-positive NET-like structures (Fig. 5B). To check whether the NETs also contained RNA, a specifically RNA-selective fluorescent dye, SYTO RNAselect [34], was used to stain NETs. This staining showed released endogenous RNA (green) in both PMA and RNA-LL37-mediated NETs (Fig. 5B). Of note, RNA staining but not DNA staining, was sensitive to RNase A (Fig. S5A, B). Additionally, the extracellular signal could be attributed to released 'cellular RNA' and distinguished from the exogenously added 'stimulant RNA' by using AF647-labeled RNA for stimulation (Fig. S5C). The same applied to LL37, using Atto488-LL37 (Fig. S5D). To exclude artefacts that might arise from staining fixed samples, RNA-LL37 mediated NETosis was also analyzed and confirmed using live-cell time-lapse analysis of PMNs (Fig. 5C and Movies S1-S3, quantified in Fig. 5D). Interestingly, in PMNs captured on the verge of NETosis, RNA staining in a granula-like fashion could be clearly observed (Fig. S5E). Thus, RNA-LL37 activates primary PMN to release NETs that contain further RNA in addition to DNA and LL37. Increased levels of NETs containing DNA have already been reported in the blood and skin of psoriasis patients [35]. To check whether this was also the case for RNA, we stained skin sections with SYTO RNAselect, anti-LL37 and anti-NE Abs. As expected psoriatic skin was highly positive for LL37 but also the RNA signal was generally stronger when compared to healthy skin, using identical staining and microscopy settings (Fig. 5E). RNA and LL37 were not always fully co-localized but were rather observed in each other's proximity. However, in samples with high PMN infiltration (anti-NE staining), areas of defined RNA-LL37 co-localization in proximity of PMNs were readily discernible (Fig. 5F). This may indicate that RNA-LL37 complexes could be physiologically relevant activators in psoriatic skin. Collectively, RNA-LL37 complexes were found to prompt the release of more RNA-LL37 by NETosis of PMNs, providing the requirements for a self-propagating feed forward loop of immune activation that might apply to skin PMNs.

Inhibitory oligonucleotides are able to block neutrophil responses to RNA-LL37 complexes

We next wondered whether PMN activation by RNA-LL37 could be blocked at the level of TLR activation by so-called inhibitory oligonucleotides (iODNs). IRS869, IRS661 and IRS954 represent such TLR7 and 9-inhibitory iODNs that were recently proposed for the treatment of another autoimmune disease, namely systemic lupus erythematosus (SLE), whereas IRS546 was used as a non- 'control' ODN inhibitory [36, 37, 38, 39]. Given the similarities between endosomal TLRs [40], we speculated that some of these iODNs could potentially also block TLR8, but the effects of iODNs on this receptor have not been studied systematically. In HEK293T cells exogenously expressing TLR7, TLR8 or TLR9 (control) upon transfection [40], IRS869 and IRS954 blocked NF-κB activation in response to R848 for TLR7 and 8 (Fig. 6A,B) and CpG for TLR9 (Fig. S6A). IRS661 effectively blocked TLR7- but not TLR9-mediated activation. Surprisingly, IRS661 strongly increased R848-mediated NF-κB activation via TLR8 (Fig. 6B), similar to observations made for T-rich ODNs combined with R848 [41] and highlighting the differences between R848 and RNA reported previously [40]. However, for RNA complexed with DOTAP (a synthetic complexing agent promoting endosomal uptake [42], similarly to LL37), all three iODNs blocked TLR8-mediated NF-κB activation (Fig. 6C). As the 'control' ODN IRS546 blocked NF-κB activation in response to TLR7-9 stimulation, in our hands it did not represent a proper control unlike previously published [39]. Nevertheless, the effects of all iODNs seemed specific for endosomal TLR signaling as the effect of all iODNs on NF-κB activity induced by TNF (a non-TLR receptor pathway activating NF-κB, Fig. S6B) or MyD88 overexpression (TLR receptor-independent NF-κB activation, Fig. S6C) were minor. Having excluding a toxic effect on primary PMNs (Fig. S6D), we investigated whether the observed effects could be transferred to endogenous TLR8 activation in primary PMNs. Here, we found that iODNs IRS661 and IRS954 were able to inhibit IL-8 release by primary PMNs from healthy donors in response to RNA-LL37 at nanomolar concentrations (Fig. 6D), whereas LPS-mediated IL-8 release was unaffected (Fig. S5E and Ref. 43). The blocking effect extended to MIP-1β (Fig. 6E), similar to the effect observed for chloroquine (Fig. S6F). Whereas in our hands the NE release assay was not sensitive to iODN (not shown), a preliminary experiment comparing WT and *Unc93b1*-deficient mice indicated that NETosis induced by bacterial RNA+LL37 is endosomal TLR-dependent (not shown) and thus potentially targetable via iODNs. These preliminary results await confirmation but would be in agreement with the observed TLR8-dependence and iODN-mediated inhibition of NETosis in HIV infections [43]. In conclusion, known pre-clinical iODNs are able to block RNA-LL37-mediated cytokine release.

Discussion

Although systemic therapies with biologicals have brought benefit for many psoriasis patients in industrialized countries [2], psoriasis remains a significant health problem worldwide. One reason is that triggers and mechanisms leading to disease chronification, exacerbation and flare-ups are not well understood. This uncertainty also applies to the role of PMNs in these processes [4]. Since PMNs can release nucleic acids, constitute the main sources of LL37 in humans and congregate in psoriatic skin, we chose to study PMN RNA-LL37-mediated responses after identifying TLR8 as an RNA receptor on PMNs [18]. We now provide novel evidence that RNA-LL37 can directly activate PMNs to release chemo-/cytokines and NETs, and that NET RNA could serve as a novel immunostimulatory component within NETs, which has not been appreciated so far. Interestingly, insect NETs contain primarily RNA rather than DNA [44], and eosinophils pre-store RNA within their granules [45]. RNA may thus be a common and functionally important NET component but this remains to be explored further. Given that RNA can also amplify responses to other PRR ligands[46], the role of RNA will thus be interesting to explore in other NET-related disease, e.g. SLE [47], atherosclerosis [48] and even cancer [49], where the focus so far has been largely on DNA.

Recently, the effects of DNA-/RNA-LL37 complexes on pDCs were reported as a novel mechanism in psoriasis inflammation [8, 9]. However, since pDC are only a minor cell population even in psoriatic skin and they cannot release nucleic acids, their contribution to cell-mediated inflammation and the provision of self-ligands should be restricted to amplifying an already ongoing pathology, characterized by pDC-attracting chemokines and an existing presence of self-ligands in the skin. We found that the combination of RNA and LL37 produces an inflammatory ligand that is not only sensed by PMNs; it also prompted the release of further components for additional RNA-LL37 and DNA-LL37 complexes. Whereas for pDCs both "inflammatory ingredients", RNA or DNA and LL37, will need to be provided by another cellular source first, a small number of activated and NETing PMNs – by releasing both, LL37 and RNA/DNA – may spark potent, self-propagating inflammation *inter pares* and *in situ.* Following an initial activation of PMN by endogenous RNA from damaged skin cells (so-called Köbner phenomenon) or by bacterial RNA [27] (*cf.* Fig. 1K) immune activation may get out of control due to chemokine release and NET formation (and thus nucleic acid and LL37 extrusion [50]) which has been observed in the skin of psoriasis patients [35]. Although the concentration of PMN cytokines measured after 4 h stimulation was moderate, release over longer time periods and the sheer number of PMNs found in psoriatic skin may nevertheless contribute substantially to local inflammation and attraction of additional leukocytes over time. The PMN-mediated ongoing release of NET DNA, RNA and LL37 would eventually enable pDCs to join the vicious cycle of activation fueled by endogenous nucleic acids [8, 9]. Additionally, cytokine-mediated inflammation is known to favor KC hyper-proliferation [51], LL37 production [52], TLR9 responsiveness [53] and IFN production [54], as well as T

cell and monocyte attraction and polarization [12] (Fig. S7). In conclusion, our study provides a plausible explanation how PMNs may contribute to early disease development and, based on the observed effects of iODNs on PMN activation, warrants the further exploration of TLR pathways and PMNs as targets for restricting innate immune activation in psoriatic skin.

Methods

Reagents

All chemicals were from Sigma unless otherwise stated. PRR agonists and LL37 were from Invivogen except RNA40 (iba Lifescience, normal and AF647-labeled) and CpG PTO 2006 (TIB Molbiol), see Table S2 and 3. iODNs used in this study with their respective sequences are listed in Table S3 and were from TIB Molbiol. Total human mRNA was isolated from HEK293T cells using the RNeasy kit on a QIAcube, both from QIAGEN. *S. aureus* RNA was isolated as described [21]. Genomic human DNA was isolated from whole blood using QIAamp DNA Blood Mini Kit from Qiagen (51106) and phosphodiester DNA from TIB Molbiol. LL37 was from InvivoGen (see Table S2) and DOTAP from Roth, L787.2. LL37 was Atto488 (from Atto-Tec as a carboxy-reactive reagent)-labeled using standard procedures. For complex formation 5.8 µM RNA40 (approximately 34.4 µg/ml and equimolar to R848 used in this setting), 1 µM ssDNA (approximately 20 µg/ml and equimolar to CpG used in this setting, sequence see Table S3), genomic DNA (20 µg/ml) or bacterial RNA (20 µg/ml) was mixed together with 10 µg LL37 (see Table S2, Atto-488 where indicated) and left for one hour at RT. For the RNA-only or LL37-only conditions, the same amounts and volumes were used replacing one of the constituents by sterile, endotoxin-free H_2O. Ficoll was from Millipore. Antibodies used for flow cytometry, ImageStream analysis or fluorescence microscopy are listed in Table S4 as well as the recombinant cytokines used in this study. Constructs used for HEK293T transfection are listed in Table S5.

Study participants and sample acquisition

All patients and healthy blood donors included in this study provided their written informed consent before study participation. Approval for use of their biomaterials was obtained by the local ethics committees at the University Hospitals of Tübingen and Heidelberg, in accordance with the principles laid down in the Declaration of Helsinki as well as applicable laws and regulations. All blood or skin samples obtained from psoriasis patients (median age 41.8 years, PASI >10, no systemic treatments at the time of blood/skin sampling) were obtained at the University Hospitals Tübingen or Heidelberg, Departments of Dermatology, respectively, and were processed simultaneously with samples from at least one healthy donor matched for age and sex (recruited at the University of

Tübingen, Department of Immunology). Skin sections were from 6 patients with Plaque Psoriasis and 1 Patient with Psoriasis guttata.

Mice and isolation of bone-marrow derived PMN (BM-PMN)

Unc93b1$^{3d/3d}$ mice [55] (C57BL/6 background, from K. Kirschning, Essen University, Germany) and WT C57BL/6 mice between 8 and 20 weeks of age were used, in accordance with local institutional guidelines on animal experiments and under specific locally approved protocols for sacrificing and *in vivo* work. All mouse colonies were maintained in line with local regulatory guidelines and hygiene monitoring. Bone-marrow (BM)-PMNs were isolated from the bone marrow using magnetic separation (mouse Neutrophil isolation kit, Miltenyi Biotec, 130-097-658) and following the manufacturer's instructions. PMN stimulation was carried out for 5 hours at 37 °C and 5% CO_2. Thereafter supernatants were harvested and used for ELISA or the cells were stained for microscopy.

Neutrophil isolation and stimulation

Whole blood (EDTA-anticoagulated) was diluted in PBS (Thermo Fisher, 14190-169), loaded on Ficoll (1.077 g/ml, Biocoll, ab211650) and centrifuged for 25 min at 366 x g at 21 °C without brake. All layers were discarded after density gradient separation except for the erythrocyte-granulocyte pellet. Thereafter, erythrocyte lysis (using 1x ammonium chloride erythrocyte lysis buffer, see Table S6) was performed twice (for 20 and 10 min) at 4 °C on a roller shaker. The remaining cell pellet was carefully resuspended in culture medium (RPMI culture medium (Sigma Aldrich, R8758) + 10% FBS (heat inactivated, TH Geyer, 11682258)) and 1.6 x 10^6 cells/ml were seeded (24 well plate, 96 well plate). After resting for 30 min at 37°C, 5% CO_2, the cells were pre-treated with inhibitors (where indicated) for 30 min and subsequently stimulated with the indicated agonists for 4 hours (for ELISA) or for 30 min to 3 h (for FACS analysis or microscopy).

PBMC isolation

Whole blood (EDTA anticoagulant) was diluted in PBS. After density gradient separation using Ficoll (described above), the PBMC layer was then carefully transferred into a new reaction tube and diluted in PBS (1:1). The cell suspension was spun down at 1800 rpm for 8 min. The cells were then washed twice more in PBS, resuspended in culture medium (RPMI + 10% FBS (heat inactivated) + 1% L-glutamine), before counting and seeding.

Flow cytometry

After PMN isolation and stimulation, the purity and activation status of neutrophils was determined by flow cytometry. 200 µl of the cell suspension was transferred into a 96 well plate (U-shape) and spun down for 5 min at 322 x g, 4 °C. FcR block was performed using pooled human serum diluted 1:10 in FACS buffer (PBS, 1 mM EDTA, 2% FBS heat inactivated) for 15 min at 4 °C. After washing, the

samples were stained for approximately 20-30 min at 4°C in the dark. Thereafter, fixation buffer (4% PFA in PBS) was added to the cell pellets for 10 min at RT in the dark. After an additional washing step, the cell pellets were resuspended in 150 µl FACS buffer. Measurements were performed on a FACS Canto II from BD Bioscience, Diva software. Analysis was performed using FlowJo V10 analysis software.

ELISA

Cytokines were determined in half-area plates (Greiner, Bio-one) using duplicates or triplicates and measuring with a standard plate reader. The assays were performed according to the manufacturer's instructions (Biolegend, R&D systems), using appropriate dilutions of the supernatants. For LL37 determination a kit from HycultBiotech (HK321-02) was used following the manufacturer's instructions.

ImageStream analysis

ImageStream analysis was used to analyze internalization of RNA-LL37 complexes using spot-counts and tracking single cells. The cells were first seeded in a 96 well plate, 8 x 10^6 cells/ml, 125 µl per well. Subsequently, they were stimulated for 1 hour with RNA-AF647 (IBA technologies) and/or LL37-Atto488 (kindly provided by Hubert Kalbacher, University of Tübingen). FcR block and surface staining (here CD15 PE) was performed as described above. After fixation, the cells were permeabilized with 0.05 % Saponin (Applichem, A4518.0100) for 15 min at RT in the dark. After washing, nuclei were stained with Hoechst 33342 (Sigma, B2261, 1 µg/ml) for 5 min at RT in the dark, washed and resuspended in 50 µl FACS buffer and transferred into a 1.5 ml Eppendorf tube. At least 10.000 cells were acquired for each sample with 40x magnification using an ImageStream X MKII with the INSPIRE instrument controller software (Merck-Millipore/Amnis). Data were analyzed with IDEAS Image analysis software. All samples were gated on single cells in focus.

Fluorescence Microscopy of fixed neutrophils

The cells were seeded in a 96 well plate at 1.6 x 106 cells/ml, 125 µl per well. Subsequently they were stimulated with the complexes for 30 min and 1 hour using RNA-AF647 and/or LL37-Atto488. FcR block, staining, fixation and permeabilization were performed as for Flow cytometry. The cell pellets were resuspended in 50-100 µl FACS buffer. 40 µl of the cell suspension was pipetted on a Poly-L-Lysine coated coverslip (Corning, 734-1005) and the cells were left to attach for one hour in the dark. ProLong Diamond Antifade (Thermo Fisher, P36965) was used to mount the coverslips on uncoated microscopy slides. For NET analysis PMNs were seeded in 24 well plates, containing Poly-L-Lysine coated coverslips and stimulated with RNA-LL37 complexes or PMA (600 nM) for 3 hours. NETs were fixed and stained using the protocol from Brinkmann et al.[56]. Where indicated, 100 µg/ml RNase A (DNase, protease-free, ThermoFisher, EN0531) was added after fixation and incubated overnight at

37°C. RNA was stained using SYTO RNAselect Green fluorescent dye (Thermo Fisher, 50 µM) and nuclear DNA was stained with Hoechst33342 (Thermo Fisher, 1 µg/ml). LL37 and PMNs were visualized using an unconjugated rabbit anti-LL37 antibody or unconjugated mouse anti-NE with subsequent staining with an AF647-conjugated anti-rabbit or an AF594-conjugated anti-mouse antibody, respectively (see Supplementary Table S4), after blocking with pooled human serum (1:10 in PBS). Secondary antibodies alone did not yield any significant staining. The slides were left to dry overnight at RT in the dark and were then stored at 4 °C before microscopy. The measurements were conducted with a Nikon Ti2 eclipse (100x magnification) and the analysis was performed using Fiji analysis software.

Fluorescence Microscopy of tissue samples

Skin samples from Psoriasis patients with a PASI ≥ 10 and without systemic treatment, and healthy skin samples paraffin-embedded according to standard procedures were deparaffinized and rehydrated using Roti Histol (Roth, 6640.1) and decreasing concentrations of ethanol (100%, 95%, 80% and 70%). After rinsing in ddH_2O, antigen retrieval was performed by boiling for 10-20 min in citrate buffer (0.1 M, pH=6). The skin tissue was then washed 3 times for 5 min with PBS. Blocking was performed using pooled human serum (1:10 in PBS) for 30 min at RT. The primary antibody was added either overnight at 4°C or for 1 hour at RT. After 3 washes, the secondary antibody was added for 30 min at RT in the dark. After another 3 washes, SYTO RNAselect Green fluorescent dye (Thermo Fisher, 50 µM) was added for 20 min at RT in the dark. Thereafter, the samples were washed again and Hoechst 33342 (ThermoFisher, 1 µg/ml) was added for 5 min. Then 3 last washes were performed before using ProLong Diamond Antifade (Thermo Fisher, P36965) for mounting. The samples were left to dry overnight at RT in the dark before being used for microscopy or stored at 4°C. The specimens were analyzed on a Nikon Ti2 eclipse bright-field fluorescence microscope (10x-40x magnification) and the analysis was performed using Fiji analysis software.

Live cell imaging of primary neutrophils

Human neutrophils were isolated by magnetic separation using MACSxpress whole blood neutrophil isolation kit (Miltenyi Biotec, 130-104-434) and were seeded into a micro-insert 4 well dish (Ibidi 80406). Hoechst 33342 (1 µg/ml) and SYTO RNAselect Green fluorescent dye (50 µM) were added to the cells and incubated for 20 min at 37°C, 5 % CO_2. Live cell imaging was performed by using Nikon Ti2 eclipse bright-field fluorescence microscope (40x magnification) including a CO2-O2 controller from Okolab. Measurements were started immediately after adding of stimuli. Time-lapse analysis was performed by taking pictures every 3 min for at least 2 hours. Image analysis was performed using NIS Elements from Nikon and Fiji analysis software.

Luminex cytokine multiplex analysis

All samples were stored at -70 °C until testing. The samples were thawed at room temperature, vortexed, spun at 18,000 x g for 1 min to remove debris and the required sample volumes were removed for multiplex analysis according to the manufacturer's recommendations. The samples were successively incubated with the capture microspheres, a multiplexed cocktail of biotinylated, reporter antibodies, and a streptavidin-phycoerythrin (PE) solution. Analysis was performed on a Luminex 100/200 instrument and the resulting data were interpreted using proprietary data analysis software (Myriad RBM). Analyte concentrations were determined using 4 and 5 parameter, weighted and non-weighted curve fitting algorithms included in the data analysis package.

Cytometric bead array

A cytometric bead array was performed using the "Human inflammatory cytokine kit" from BD Bioscience (551811) and following the manufacturer's instruction. 25 µl of samples and standards were added to 25 µl of the capturing bead mixture. Additionally, 25 µl of PE detection reagent was added to all tubes and incubated for 3 h at RT in the dark. Thereafter, 1 ml of wash buffer was added to each tube and centrifuged at 200 x g for 5 minutes. The supernatant was carefully removed and the pellet was resuspended in 300 µl wash buffer. Measurements were performed with the FACS Canto II from BD Bioscience operated using Diva software. Analysis was performed with Soft Flow FCAP Array v3 analysis software from BD Bioscience.

Transwell experiments

PBMCs and Neutrophils were always used from the same donor in each experiment. Transwell inserts were loaded with 100 µl of PBMC suspension (0.8 x 10^6 cells/insert). In the lower chamber, either PMNs were seeded as described above (same plate size, same volume, same cell concentration) using polycarbonate, 24 well plates, 3 µm pores, Corning, 734-1570) and stimulated for 4 h with stimuli as indicated. Alternatively, media containing the stimuli only (i.e. no PMNs) or media containing only MIP-1β (30 and 150 pg /ml), IL-16 (300 and 1500 pg/ml) or SDF-1α (control, 100 ng/ml) and no PMNs were added. After 4 h, the lower compartment was harvested and FACS staining was performed as described above. The total number of migrated cells was acquired using counting beads (Biolegend, 424902) on a FACS Canto II (BD Bioscience) with Diva software. Analysis was performed using FlowJo V10 analysis software.

Neutrophil elastase NETosis assay

Neutrophil extracellular trap formation was determined using the colorimetric NETosis Assay Kit from Cayman Chemicals based on the enzymatic activity of NET-associated neutrophil elastase. PMNs from various healthy donors were isolated as described above and stimulated with RNA-LL37 complex, or PMA and a calcium ionophore (A-23187) as positive controls for 1 or 3 hours. The assay was

performed following the manufacturer's instructions. The absorbance was then measured at 405 nm using a standard plate reader.

Transient transfection of HEK293T cells

HEK293T cells were transiently transfected using the $CaPO_4$ method as described [40]. Cells were seeded in 24-well plates at a density of 14 x 10^5 cells/ml 2-3 h prior to transfection. For the transfection of one well, 310 ng of plasmid DNA (100 ng TLR plasmid, 100 ng firefly luciferase NF-κB reporter, 10 ng *Renilla* luciferase control reporter, and 100 ng EGFP plasmid) was mixed with 1.2 µl of a 2 M $CaCl_2$ solution and filled up with sterile endotoxin-free H_20 to obtain a total reaction volume of 10 µl. After the addition of 10 µl of 2X HBS solution (50 mM HEPES (pH 7.05), 10 mM KCl, 12 mM Glucose, 1.5 mM Na_2HPO_4), the mixture was then added to the cell suspension. As negative controls, TLR coding plasmids were replaced by empty vectors carrying the appropriate backbone of the TLR plasmids. After the addition of the transfection complexes, the cells were incubated either for 24 h followed by stimulation, or kept for 48 h without stimulation (MyD88 expression). For stimulation, the media was aspirated and replaced by fresh growth medium in which TNFα or the different TLR ligands (R848, CpG, RNA40) with or without IRS were diluted to appropriate concentrations. TLR8 activation with RNA40 was facilitated by complexation of the RNA with DOTAP (L787.1, Roth). RNA40 and DOTAP were first diluted in 1X HBS separately. Next, RNA40/HBS was diluted 1:3 in DOTAP/HBS. The solution was carefully mixed by pipetting up and down. After 15 min of incubation at RT, the mixture was 1:6.7 diluted in growth medium (with or without IRS) and finally dispensed (500 µl/well) into the wells containing transfected HEK293T cells. Each tested condition was measured in triplicates. The cells were stimulated and inhibited for 24 h at 37°C.

Dual Luciferase Reporter Assay

After checking transfection efficiency via EGFP fluorescence microscopy, HEK293T supernatants were aspirated and 60 µl of 1X passive lysis buffer (E194A, Promega) added per well. The plate was then incubated for 15 min at RT on the plate shaker and subsequently stored at -80 °C for at least 15 minutes to facilitate complete cell lysis. After thawing, 60 µl were transferred into a V-bottom 96-well plate and centrifuged for 10 min at 2500 rpm and 4 °C to pellet cell debris. 10 µl supernatant were then transferred into a white microplate and each condition was measured in triplicates using the FLUOstar OPTIMA device (BMG Labtech). Firefly and Renilla luciferase activity were determined using the Promega Dual luciferase kit. Both enzyme activities were measured for 12.5 s with 24 intervals of 0.5 s, respectively. The data was analyzed by calculating the ratio of the two measured signals, thereby normalizing each firefly luciferase signal to its corresponding Renilla luciferase signal. The ratios were represented as the relative light units (RLU) of NF-κB activation.

Statistics

Experimental data was analyzed using Excel 2010 (Microsoft) and/or GraphPad Prism 6 or 7, microscopy data with ImageJ/Fiji, flow cytometry data with FlowJo 10. In case of extreme values, outliers were statistically identified using the ROUT method at high (0.5%) stringency and normality tested using the Shapiro-Wilk test for the subsequent choice of a parametric or non-parametric test. p-values (α=0.05) were then calculated and multiple testing was corrected for in Prism, as indicated in the figure legends. Values < 0.05 were generally considered statistically as significant and denoted by * throughout. Comparisons made to unstimulated control, unless indicated otherwise, denoted by brackets.

References

1. Griffiths CE, Barker JN. Pathogenesis and clinical features of psoriasis. *Lancet* **370**, 263-271 (2007).

2. Eberle FC, Bruck J, Holstein J, Hirahara K, Ghoreschi K. Recent advances in understanding psoriasis. *F1000Res* **5**, (2016).

3. Sen BB, Rifaioglu EN, Ekiz O, Inan MU, Sen T, Sen N. Neutrophil to lymphocyte ratio as a measure of systemic inflammation in psoriasis. *Cutan Ocul Toxicol*, (2013).

4. Schon MP, Broekaert SM, Erpenbeck L. Sexy again: the renaissance of neutrophils in psoriasis. *Exp Dermatol* **26**, 305-311 (2017).

5. Morizane S, Gallo RL. Antimicrobial peptides in the pathogenesis of psoriasis. *J Dermatol* **39**, 225-230 (2012).

6. Sorensen O, Arnljots K, Cowland JB, Bainton DF, Borregaard N. The human antibacterial cathelicidin, hCAP-18, is synthesized in myelocytes and metamyelocytes and localized to specific granules in neutrophils. *Blood* **90**, 2796-2803 (1997).

7. Lande R*, et al.* The antimicrobial peptide LL37 is a T-cell autoantigen in psoriasis. *Nat Commun* **5**, 5621 (2014).

8. Lande R*, et al.* Plasmacytoid dendritic cells sense self-DNA coupled with antimicrobial peptide. *Nature* **449**, 564-569 (2007).

9. Ganguly D*, et al.* Self-RNA-antimicrobial peptide complexes activate human dendritic cells through TLR7 and TLR8. *The Journal of experimental medicine* **206**, 1983-1994 (2009).

10. Afshar M, Martinez AD, Gallo RL, Hata TR. Induction and exacerbation of psoriasis with Interferon-alpha therapy for hepatitis C: a review and analysis of 36 cases. *J Eur Acad Dermatol Venereol* **27**, 771-778 (2013).

11. Yao Y*, et al.* Type I interferon: potential therapeutic target for psoriasis? *PLoS One* **3**, e2737 (2008).

12. Ghoreschi K, Weigert C, Rocken M. Immunopathogenesis and role of T cells in psoriasis. *Clin Dermatol* **25**, 574-580 (2007).

13. Terui T, Ozawa M, Tagami H. Role of neutrophils in induction of acute inflammation in T-cell-mediated immune dermatosis, psoriasis: a neutrophil-associated inflammation-boosting loop. *Experimental dermatology* **9**, 1-10 (2000).

14. Kruger P*, et al.* Neutrophils: Between host defence, immune modulation, and tissue injury. *PLoS Pathog* **11**, e1004651 (2015).

15. Tecchio C, Micheletti A, Cassatella MA. Neutrophil-derived cytokines: facts beyond expression. *Front Immunol* **5**, 508 (2014).

16. Brinkmann V*, et al.* Neutrophil extracellular traps kill bacteria. *Science* **303**, 1532-1535 (2004).

17. Radic M, Marion TN. Neutrophil extracellular chromatin traps connect innate immune response to autoimmunity. *Seminars in immunopathology* **35**, 465-480 (2013).

18. Berger M*, et al.* Neutrophils express distinct RNA receptors in a non-canonical way. *The Journal of biological chemistry* **287**, 19409-19417 (2012).

19. Lindau D*, et al*. Primary blood neutrophils express a functional cell surface Toll-like receptor 9. *European Journal of Immunology* **43**, 2101-2113 (2013).

20. Kawasaki T, Kawai T. Toll-like receptor signaling pathways. *Front Immunol* **5**, 461 (2014).

21. Eigenbrod T, Pelka K, Latz E, Kreikemeyer B, Dalpke AH. TLR8 Senses Bacterial RNA in Human Monocytes and Plays a Nonredundant Role for Recognition of Streptococcus pyogenes. *J Immunol* **195**, 1092-1099 (2015).

22. Janke M*, et al.* Selective and direct activation of human neutrophils but not eosinophils by Toll-like receptor 8. *The Journal of allergy and clinical immunology* **123**, 1026-1033 (2009).

23. Kuznik A, Bencina M, Svajger U, Jeras M, Rozman B, Jerala R. Mechanism of endosomal TLR inhibition by antimalarial drugs and imidazoquinolines. *Journal of Immunology* **186**, 4794-4804 (2011).

24. Schmidt NW*, et al.* Liquid-crystalline ordering of antimicrobial peptide-DNA complexes controls TLR9 activation. *Nat Mater* **14**, 696-700 (2015).

25. Matsukura S*, et al.* Role of RIG-I, MDA-5, and PKR on the expression of inflammatory chemokines induced by synthetic dsRNA in airway epithelial cells. *Int Arch Allergy Immunol* **143 Suppl 1**, 80-83 (2007).

26. Alekseyenko AV*, et al.* Community differentiation of the cutaneous microbiota in psoriasis. *Microbiome* **1**, 31 (2013).

27. Eigenbrod T, Dalpke AH. Bacterial RNA: An Underestimated Stimulus for Innate Immune Responses. *J Immunol* **195**, 411-418 (2015).

28. Eigenbrod T*, et al.* Bacterial RNA mediates activation of caspase-1 and IL-1beta release independently of TLRs 3, 7, 9 and TRIF but is dependent on UNC93B. *J Immunol* **189**, 328-336 (2012).

29. Cruikshank W, Little F. Interleukin-16: The Ins and Outs of Regulating T-Cell Activation. *Critical Reviews in Immunology* **28**, 467-483 (2008).

30. Roth S, Solbach W, Laskay T. IL-16 and MIF: messengers beyond neutrophil cell death. *Cell Death Dis* **7**, e2049 (2016).

31. Menten P, Wuyts A, Van Damme J. Macrophage inflammatory protein-1. *Cytokine Growth Factor Rev* **13**, 455-481 (2002).

32. Atanasova M, Whitty A. Understanding cytokine and growth factor receptor activation mechanisms. *Crit Rev Biochem Mol Biol* **47**, 502-530 (2012).

33. Lande R*, et al.* Neutrophils activate plasmacytoid dendritic cells by releasing self-DNA-peptide complexes in systemic lupus erythematosus. *Sci Transl Med* **3**, 73ra19 (2011).

34. Li Q*, et al.* RNA-selective, live cell imaging probes for studying nuclear structure and function. *Chem Biol* **13**, 615-623 (2006).

35. Hu SC, Yu HS, Yen FL, Lin CL, Chen GS, Lan CC. Neutrophil extracellular trap formation is increased in psoriasis and induces human beta-defensin-2 production in epidermal keratinocytes. *Sci Rep* **6**, 31119 (2016).

36. Duramad O*, et al.* Inhibitors of TLR-9 act on multiple cell subsets in mouse and man in vitro and prevent death in vivo from systemic inflammation. *J Immunol* **174**, 5193-5200 (2005).

37. Guiducci C*, et al.* TLR recognition of self nucleic acids hampers glucocorticoid activity in lupus. *Nature* **465**, 937-941 (2010).

38. Barrat FJ, Coffman RL. Development of TLR inhibitors for the treatment of autoimmune diseases. *Immunol Rev* **223**, 271-283 (2008).

39. Barrat FJ*, et al.* Nucleic acids of mammalian origin can act as endogenous ligands for Toll-like receptors and may promote systemic lupus erythematosus. *The Journal of experimental medicine* **202**, 1131-1139 (2005).

40. Colak E*, et al.* RNA and imidazoquinolines are sensed by distinct TLR7/8 ectodomain sites resulting in functionally disparate signaling events. *J Immunol* **192**, 5963-5973 (2014).

41. Jurk M*, et al.* Modulating responsiveness of human TLR7 and 8 to small molecule ligands with T-rich phosphorothiate oligodeoxynucleotides. *European Journal of Immunology* **36**, 1815-1826 (2006).

42. Yasuda K*, et al.* Endosomal translocation of vertebrate DNA activates dendritic cells via TLR9-dependent and -independent pathways. *J Immunol* **174**, 6129-6136 (2005).

43. Saitoh T*, et al.* Neutrophil extracellular traps mediate a host defense response to human immunodeficiency virus-1. *Cell Host Microbe* **12**, 109-116 (2012).

44. Altincicek B, Stotzel S, Wygrecka M, Preissner KT, Vilcinskas A. Host-derived extracellular nucleic acids enhance innate immune responses, induce coagulation, and prolong survival upon infection in insects. *J Immunol* **181**, 2705-2712 (2008).

45. Behzad AR*, et al.* Localization of DNA and RNA in eosinophil secretory granules. *Int Arch Allergy Immunol* **152**, 12-27 (2010).

46. Noll F*, et al.* Self-extracellular RNA acts in synergy with exogenous danger signals to promote inflammation. *PLoS One* **12**, e0190002 (2017).

47. Gestermann N*, et al.* Netting Neutrophils Activate Autoreactive B Cells in Lupus. *J Immunol* **200**, 3364-3371 (2018).

48. Warnatsch A, Ioannou M, Wang Q, Papayannopoulos V. Inflammation. Neutrophil extracellular traps license macrophages for cytokine production in atherosclerosis. *Science* **349**, 316-320 (2015).

49. Gregoire M*, et al.* Neutrophils trigger a NF-kappaB dependent polarization of tumor-supportive stromal cells in germinal center B-cell lymphomas. *Oncotarget* **6**, 16471-16487 (2015).

50. Neumann A*, et al.* The antimicrobial peptide LL-37 facilitates the formation of neutrophil extracellular traps. *Biochem J* **464**, 3-11 (2014).

51. Hanel KH, Cornelissen C, Luscher B, Baron JM. Cytokines and the skin barrier. *Int J Mol Sci* **14**, 6720-6745 (2013).

52. Schauber J*, et al.* Injury enhances TLR2 function and antimicrobial peptide expression through a vitamin D-dependent mechanism. *The Journal of clinical investigation* **117**, 803-811 (2007).

53. Morizane S*, et al.* Cathelicidin antimicrobial peptide LL-37 in psoriasis enables keratinocyte reactivity against TLR9 ligands. *The Journal of investigative dermatology* **132**, 135-143 (2012).

54. Zhang LJ*, et al.* Antimicrobial Peptide LL37 and MAVS Signaling Drive Interferon-beta Production by Epidermal Keratinocytes during Skin Injury. *Immunity* **45**, 119-130 (2016).

55. Tabeta K*, et al.* The Unc93b1 mutation 3d disrupts exogenous antigen presentation and signaling via Toll-like receptors 3, 7 and 9. *Nature Immunology* **7**, 156-164 (2006).

56. Brinkmann V, Laube B, Abu Abed U, Goosmann C, Zychlinsky A. Neutrophil extracellular traps: how to generate and visualize them. *J Vis Exp*, (2010).

Acknowledgements

We thank H. Kalbacher, S. Pöschel, J. Berger, S. Haen, K. Preissner, O. Sorensen and A. Dalpke for provision of reagents, samples, technical support and/or helpful discussions and all healthy donors and patients for participation in our study. This study was supported by the Deutsche Forschungsgemeinschaft (German Research Foundation, DFG) CRC TR156 "The skin as an immune sensor and effector organ – Orchestrating local and systemic immunity", the University of Tübingen and the University Hospital Tübingen.

Authorship contributions

F.H., Z.B., S.D., D.E., T.K. and N.S.M. performed experiments; F.H., Z.B., S.D., D.E., N.S.M. and A.N.R.W. analyzed data; M.H., M.W.L., L.F., K.S., K.G. and T.E. were involved in sample and reagent acquisition; F.H., D.H., K.G. and T.E. contributed to the conceptual development of the study; F.H. and A.N.R.W. wrote the manuscript and all authors commented on an revised the manuscript; A.N.R.W. coordinated and supervised the entire study.

Competing interests

None of the authors declare competing interests.

Materials & Correspondence

Please address requests to:

Alexander N. R. Weber, Interfaculty Institute for Cell Biology, Department of Immunology, University of Tübingen, Auf der Morgenstelle 15, 72076 Tübingen, Germany. Tel.: +49 7071 29 87623. Fax: +49 7071 29 4579. Email: alexander.weber@uni-tuebingen.de

Abbreviations

APC – antigen-presenting cell; bRNA – bacterial ribonucleic acid; Enhanced green fluorescence protein – EGFP; Human embryonic kidney – HEK; HLA – Human leucocyte antigen; iODN – inhibitory oligonucleotides; Microbe-associated molecular pattern – MAMPs; MHC – Major histocompatibility complex; Inhibitory oligodeoxynucleotides – iODNs; Interferon – IFN; Interleukin – IL; Keratinocytes –

KC; PASI – psoriasis area and severity; Plasmacytoid dendritic cells – pDCs; PMA – phorbol myristate acetate; Pattern recognition receptor – PRR; Polymorphonuclear leukocytes – PMNs; NE - Neutrophil elastase; Neutrophil extracellular trap - NET; Scanning electron microscopy – SEM; Systemic lupus erythematosus – SLE; TLR – Toll-like receptor; Tumor necrosis factor (TNF).

Figure legends

Figure 1: Human neutrophils take up and respond to RNA when complexed to LL37

(A-C) IL-8 release (ELISA, 4 h stimulation) and CD62L shedding (flow cytometry, 1 or 2h) by PMNs from healthy donors stimulated with LPS, R848 or CpG ODN (A, n=6-7), ssDNA and genomic DNA (B, n=5), or RNA40 (C, n=8), with or without LL37. (D) Electron microscopy of PMNs incubated with RNA-LL37 for 20 min (n=1). (E-G) FACS (E, n=6), ImageStream cytometry (F, G, scale bar = 10 µm) or conventional bright-field microscopy (H, n=2, scale bar = 10 µm) of PMNs incubated for 60 min with RNA-AF647 complexed with LL37 (n=6). In F the % of cells with 'internalized' features are shown (n=2, see Methods), in G selected cells from one representative donor are shown. In H unmodified LL37 was replaced with Atto488-labeled LL37, one representative donor shown. (I) as in C but including chloroquine (CQ) pre-incubation for 30 min (n=6-7). (J) and (K) as in C but using total human RNA from HEK293T cells (J, n=4-6) or bacterial RNA isolated from *S. aureus* (K, n=4) with and without LL37. A-C, E, F, I-K represent combined data (mean+SD) from 'n' biological replicates (each dot represents one donor). In D, G and H one representative of 'n' biological replicates (donors) is shown (mean+SD). * $p<0.05$ according to one-way ANOVA with Dunnett's correction (A, B, C, I, J) or Friedman test with Dunn's correction (E, K).

Figure 2: RNA-LL37 complexes promote release of multiple pro-inflammatory cytokines and chemokines

Cytometric bead array (A-C) or ELISA (D, E) for TNF (A), IL-6 (B), IL-1β (C), IL-16 (D) or MIP-1β (E) secreted from PMNs stimulated for 4 h as indicated (n=4-7). A-E represent combined data (mean+SD) from 'n' biological replicates (each dot represents one donor). * $p<0.05$ according to one-way ANOVA with Dunnett's correction (E), Kruskall-Wallis (D) or Friedman test with Dunn's correction (A-C).

Figure 3: Psoriasis PMNs are more efficiently stimulated by RNA-LL37 complexes

(A-B) ELISA of IL-8 and MIP-1β secreted from psoriasis PMNs (n=3 patients, 9 healthy controls, squares, chequered bars) or PMNs from sex-and age-matched healthy donors (n=3 patients, 10 healthy donors as controls, circles, filled bars). (C) as in A or B but ELISA for LL37 (n=4 patients, 7 healthy donors). A-C represent combined data (mean+SD) from 'n' biological replicates (each dot represents one donor/patient). * $p<0.05$ according to one-way ANOVA with Dunnett's correction.

Figure 4: Cytokines released by human PMNs and LL37-complexed RNA induce migration of T cells and monocytes

Flow cytometric cell counts of migrated CD4 T cells (A, D), CD8 T cells (B, E) and $CD14^{+}HLA\text{-}DR^{+}$ monocytes (C, F) quantified in transwell assays with total PBMCs in the upper and either MIP-1β or IL-16 (A-C, n=6-7, $p>0.05$ for treatments vs. media) or R848, RNA with and without LL37 (D-F, n=3-7)

in the lower chamber. A-F represent combined data (mean+SD) from 'n' biological replicates (each dot represents one donor). * $p<0.05$ according to Friedmann test with Dunn's correction (A, B, D, E), or one-way ANOVA with Dunnett's correction for multiple testing (C, F).

Figure 5: RNA-LL37 trigger the release of NETs containing further RNA, DNA and LL37

(A) Neutrophil elastase (NE) release from PMNs stimulated for 3 h (n=8, each dot represents one donor). Fluorescence microscopy of fixed (B) or live (C) PMNs treated and stained as indicated (n=6 or 2). (D) Quantification of live cell microscopy (C), see also Movies S1-S3. (E, F) Skin sections from healthy (E) or psoriasis (E, F) affected skin (n=7 patients and 3 healthy controls). A and D represent combined data (mean+SD) from 'n' biological replicates. In B, C, E and F representative samples of 'n' replicates or donors are shown. Arrowheads indicate released RNA/NETs (C) or RNA-LL37 co-localization (F); * $p<0.05$ according to one-way ANOVA with Dunnett's correction (A).

Figure 6: Inhibitory oligodeoxynucleotides are able to inhibit RNA-LL37 cytokine release from human PMNs

NF-κB dual luciferase reporter assay in HEK293T cells, transfected NF-κB firefly luciferase reporter, *Renilla* control reporter and plasmids for either TLR7 (A) or TLR8 (B, C), subsequently stimulated with R848 (A, B) or RNA (C) without (arrow) or with IRS661, IRS954, IRS869 and IRS546 (0.15-3.5 µM, n=2 each). IL-8 (D, n=6) or MIP-1β (E, n=4) release from stimulated PMNs with or without IRS661 (1 nM) or IRS954 (50 nM) pre-incubation (30 min) quantified by ELISA. D and E represent combined data (mean+SD) from 'n' biological replicates (each dot represents one donor). In A-C one representative of 'n' replicates is shown (mean+SD of technical triplicates). * $p<0.05$ according to two-way ANOVA with Dunnett correction for multiple testing (A-C, comparison against 'no inhibitor' condition, arrow), one-way ANOVA with Sidak correction (D) or Friedmann test with Dunn correction (E).

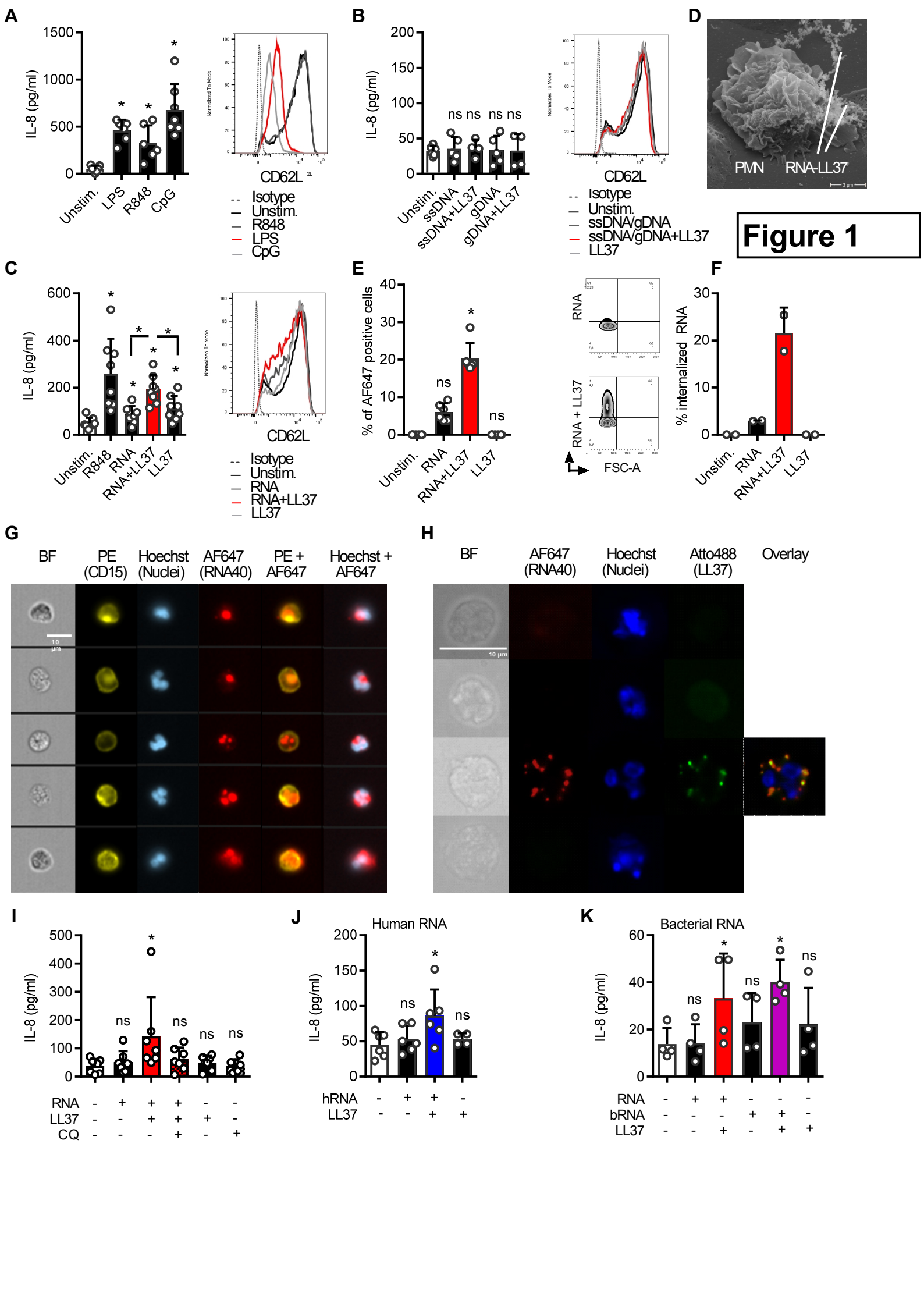
A
IL-8 (pg/ml)
1500
1000
500
0
Unstim.
LPS
R848
CpG
CD62L
Isotype
Unstim.
R848
LPS
CpG
B
IL-8 (pg/ml)
200
150
100
50
0
ns ns ns ns
Unstim.
ssDNA
ssDNA+LL37
gDNA
gDNA+LL37
CD62L
Isotype
Unstim.
ssDNA/gDNA
ssDNA/gDNA+LL37
LL37
D
PMN
RNA-LL37
Figure 1
C
IL-8 (pg/ml)
600
400
200
0
Unstim.
R848
RNA
RNA+LL37
LL37
CD62L
Isotype
Unstim.
RNA
RNA+LL37
LL37
E
% of AF647 positive cells
40
30
20
10
0
ns
ns
Unstim.
RNA
RNA+LL37
LL37
RNA
RNA + LL37
FSC-A
F
% internalized RNA
30
20
10
0
Unstim.
RNA
RNA+LL37
LL37
G
BF
PE (CD15)
Hoechst (Nuclei)
AF647 (RNA40)
PE + AF647
Hoechst + AF647
10 µm
H
BF
AF647 (RNA40)
Hoechst (Nuclei)
Atto488 (LL37)
Overlay
10 µm
I
IL-8 (pg/ml)
500
400
300
200
100
0
ns
ns
ns
ns
RNA - + + + - -
LL37 - - + + + -
CQ - - - + - +
J
Human RNA
IL-8 (pg/ml)
200
150
100
50
0
ns
ns
hRNA - + + -
LL37 - - + +
K
Bacterial RNA
IL-8 (pg/ml)
60
40
20
0
ns
ns
ns
RNA - + + - - -
bRNA - - - + + -
LL37 - - + - + +

Figure 2

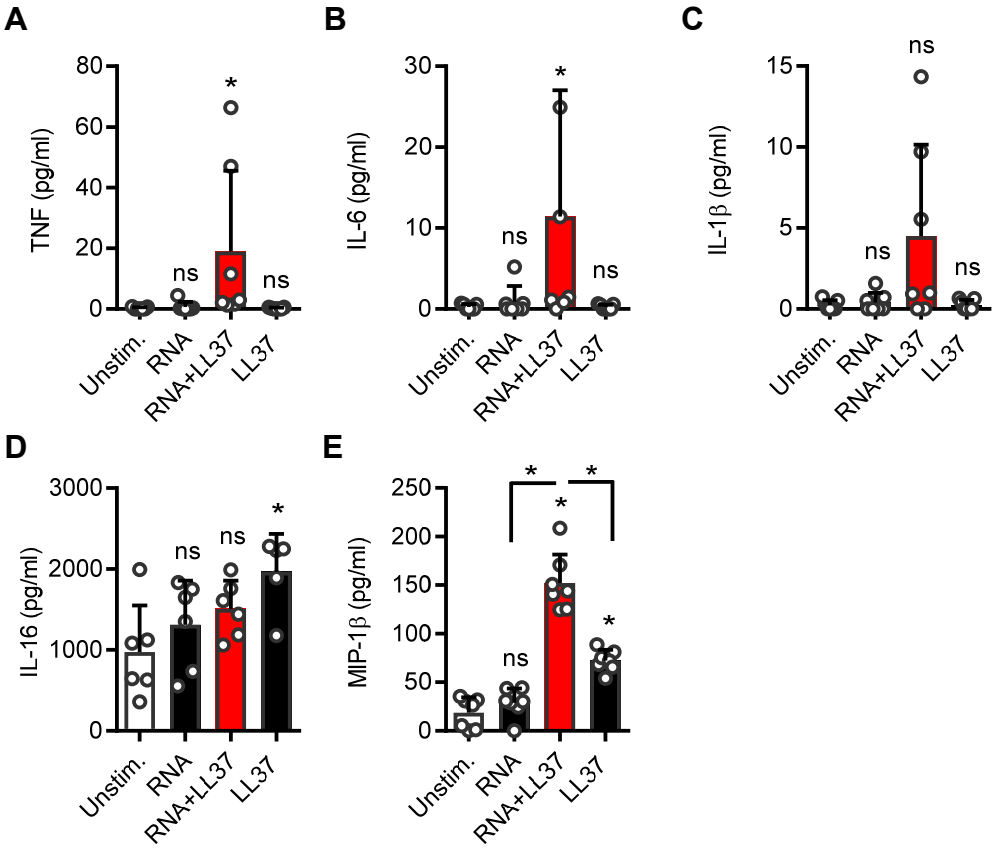
A
TNF (pg/ml)
80
60
40
20
0
ns
*
ns
Unstim.
RNA
RNA+LL37
LL37
B
IL-6 (pg/ml)
30
20
10
0
ns
*
ns
Unstim.
RNA
RNA+LL37
LL37
C
IL-1β (pg/ml)
15
10
5
0
ns
ns
ns
Unstim.
RNA
RNA+LL37
LL37
D
IL-16 (pg/ml)
3000
2000
1000
0
ns
ns
*
Unstim.
RNA
RNA+LL37
LL37
E
MIP-1β (pg/ml)
250
200
150
100
50
0
*
*
*
ns
*
Unstim.
RNA
RNA+LL37
LL37

Figure 3

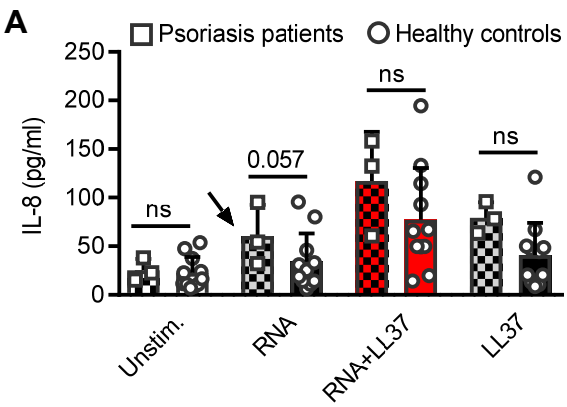
A
Psoriasis patients
Healthy controls
IL-8 (pg/ml)
250
200
150
100
50
0
ns
0.057
ns
ns
Unstim.
RNA
RNA+LL37
LL37

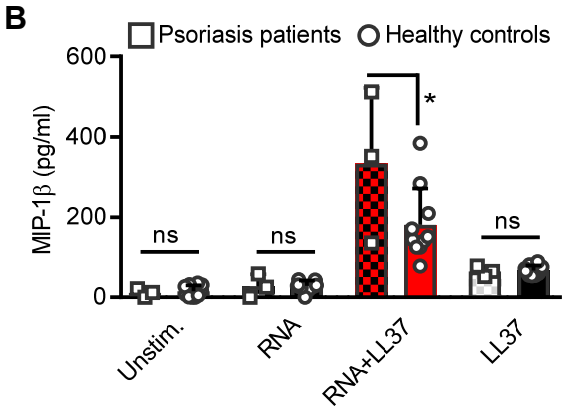
B
Psoriasis patients
Healthy controls
MIP-1β (pg/ml)
600
400
200
0
ns
ns
*
ns
Unstim.
RNA
RNA+LL37
LL37

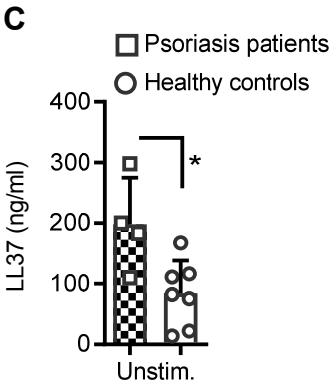
C
Psoriasis patients
Healthy controls
LL37 (ng/ml)
400
300
200
100
0
*
Unstim.

Figure 4

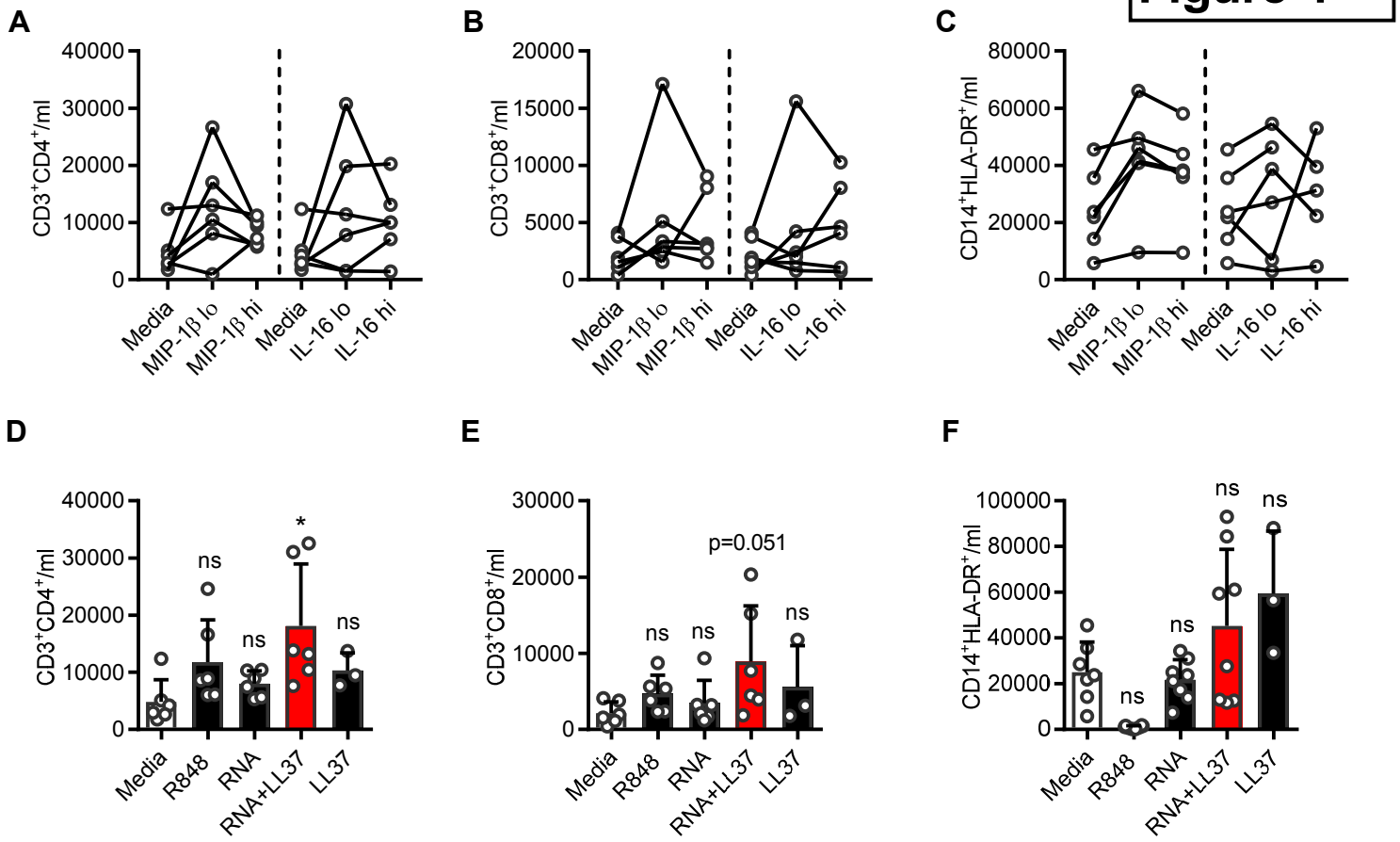
A
B
C
D
E
F
CD3+CD4+/ml
CD3+CD8+/ml
CD14+HLA-DR+/ml
Media
MIP-1β lo
MIP-1β hi
IL-16 lo
IL-16 hi
R848
RNA
RNA+LL37
LL37
ns
*
p=0.051

Figure 5

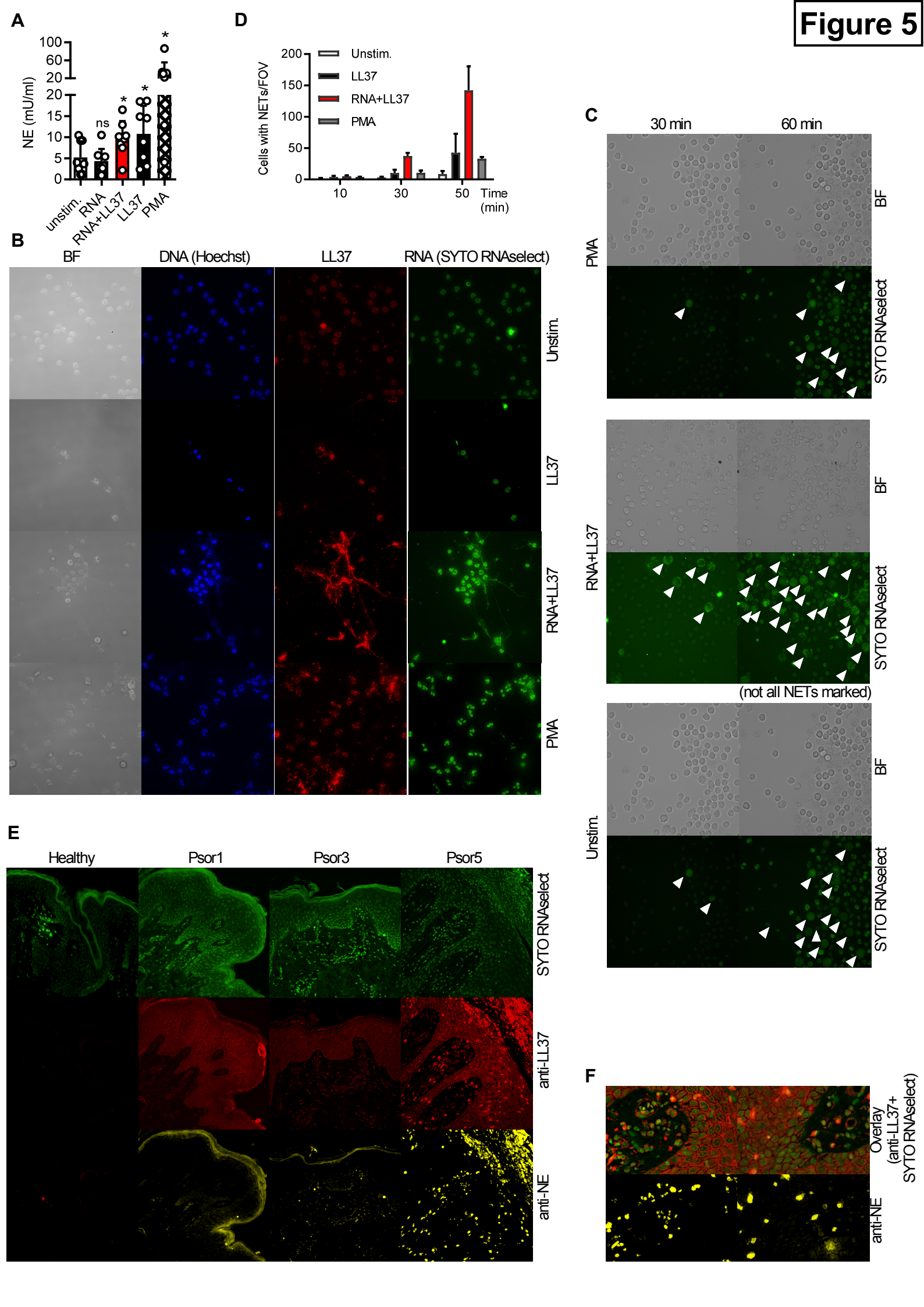
A
NE (mU/ml)
100
60
20
20
15
10
5
0
ns
*
*
*
unstim.
RNA
RNA+LL37
LL37
PMA
D
Cells with NETs/FOV
200
150
100
50
0
Unstim.
LL37
RNA+LL37
PMA
10
30
50
Time (min)
B
BF
DNA (Hoechst)
LL37
RNA (SYTO RNAselect)
Unstim.
LL37
RNA+LL37
PMA
C
30 min
60 min
PMA
BF
SYTO RNAselect
RNA+LL37
BF
SYTO RNAselect
(not all NETs marked)
Unstim.
BF
SYTO RNAselect
E
Healthy
Psor1
Psor3
Psor5
SYTO RNAselect
anti-LL37
anti-NE
F
Overlay (anti-LL37+ SYTO RNAselect)
anti-NE

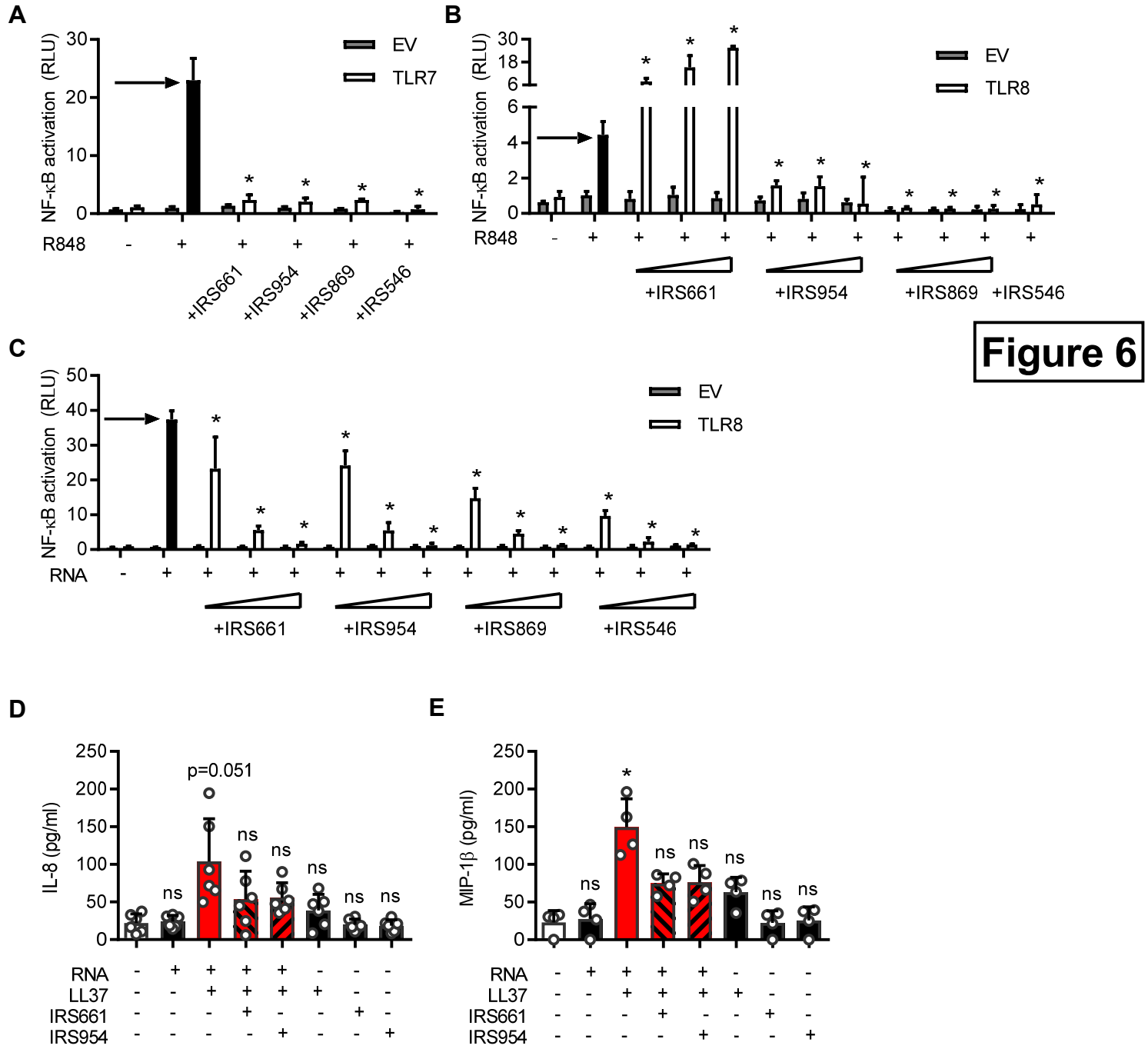
A
NF-κB activation (RLU)
EV
TLR7
R848
+IRS661
+IRS954
+IRS869
+IRS546
B
NF-κB activation (RLU)
EV
TLR8
R848
+IRS661
+IRS954
+IRS869
+IRS546
Figure 6
C
NF-κB activation (RLU)
EV
TLR8
RNA
+IRS661
+IRS954
+IRS869
+IRS546
D
IL-8 (pg/ml)
p=0.051
ns
RNA
LL37
IRS661
IRS954
E
MIP-1β (pg/ml)
ns
RNA
LL37
IRS661
IRS954

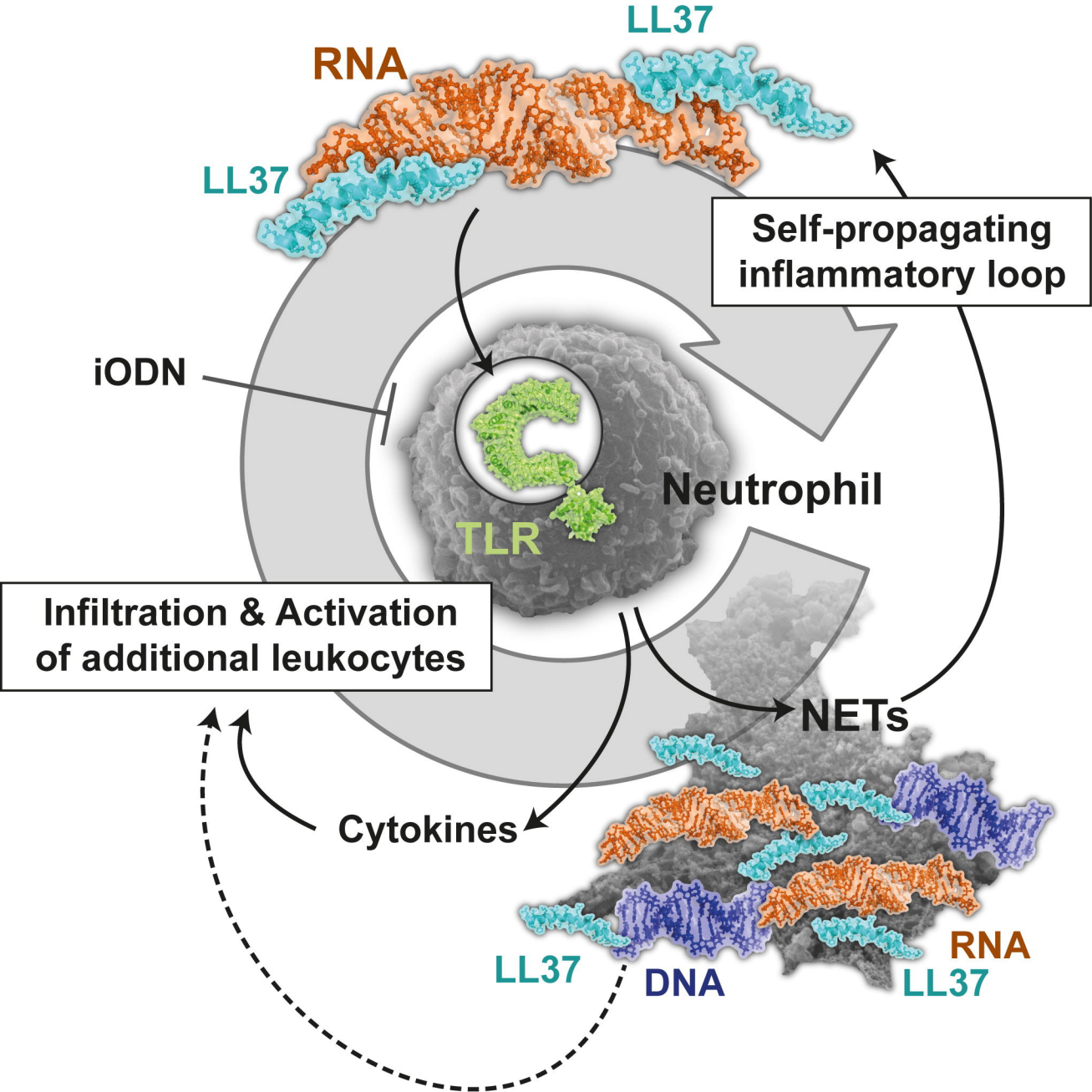
LL37
RNA
LL37
Self-propagating inflammatory loop
iODN
Neutrophil
TLR
Infiltration & Activation of additional leukocytes
NETs
Cytokines
LL37
DNA
RNA
LL37